FOCUSING MECHANISMS IN THE PULSELAC CU ACCELERATOR*

D. J. Johnson and T. R. Lockner
Sandia National Laboratories, Albuquerque, New Mexico 87185

Abstract

The post-acceleration of a 400 keV, 10 kA proton beam by a 200 kV magnetically insulated gap is investigated. The deflections from self and applied E and B fields are measured and compared to calculated values. We find that the beam is inadequately space-charge neutralized without gas puffs in regions of applied-B field to allow efficient transport. The beam is also non-current neutralized in these regions leading to self-magnetic deflection. The applied-B field is used to focus the beam both directly as a solenoidal lens and indirectly by defining the equipotential surfaces in the accelerating gap. It is also pointed out how azimuthal asymmetries in the beam current density and cathode plasma cause beam self-field asymmetries that lead to emittance growth.

Introduction

In the Pulselac concept (see Figure 1),[1,2] an annular beam is accelerated through a series of magnetically-insulated (B_r) accelerating gaps. To allow efficient beam transport through the accelerator at current densities of many A/cm^2, it is necessary to space-charge neutralize the beam in the transport region between gaps. The neutralizing electrons and the high E-field stress on these gaps mandate that the gaps be magnetically insulated to be electrically efficient. However, the radial applied magnetic field complicates the beam transport in the accelerator because the field restricts beam space-charge and current neutralization processes.

Deflections of the beam in the gap region are caused by self and applied electric and magnetic fields. The deflections from the self fields have axisymmetric and non-axisymmetric components depending upon the uniformity of the beam. The observed deflection mechanisms can be divided into five categories:

1. unneutralized space-charge,
2. self magnetic field bending,
3. applied field solenoidal focusing
4. electrostatic focusing in the gap when the electron sheath E x B drifts through spatial nonuniformities in the beam, and
5. applied electrostatic deflections.

We examine each of these deflection mechanisms and show how the non-axisymmetric components produce emittance growth .

Electrical System

The new Pulselac injector diode was powered by a 10 Ω, 800 kV, 60 water Blumlein. The post-acceleration gap (PAG) was powered by a 12 Ω water Blumlein through four, 50 Ω cables. The post-accelerator, pulsed power system was capable of supplying a 250 kV, 15 kA, 50 ns pulse to the ferrite loaded accelerating gap.

The injector diode utilized an applied-B_r field extraction ion diode.[3] The anode was fabricated from a flat aluminum disc with epoxy filled grooves which served to produce a surface flashover anode plasma. A system of four puff valves was used to inject hydrogen gas (or air) into each B_{app}-field region in the accelerator.

*This work supported by the U. S. Department of Energy under contract DE-AC04-76-DP00789.

A cross-sectional view of the system is show in Fig. 1. The anode and cathode edges of the PAG were defined by thin walled cylinders located at 6.35 and 10.2 cm radii. The insulating-B_r field was produced by four coils mounted 5 mm outside the anode and cathode cylinders. The cylinders and/or coils could be moved in the axial direction to reposition the accelerating gap position with respect to the insulating field lines and to tilt the gap. The anode-cathode gap was typically 6 mm wide and located 50 cm downstream from the injector. Each B-field coil set had twice as many turns in the inside coil as in the outside coil to give an ~ 1/R field strength variation and keep the field lines approximately parallel in the gap.

Beam Diagnostics

The total beam current was determined using dB/dt loops, and the voltage was measured using resistive voltage monitors on the injector diode and PAG. The time integrated total beam profile was determined qualitatively with 0.25-mm-thick filtered Mylar witness plates. The directions of the beam orbits were determined with a slotted shadowbox array and similarly filtered thermally sensitive paper. The time history of the radial ion beam profile was determined at different axial positions with an array of nine magnetically insulated Faraday cups. The total beam current pulse was measured 50 cm after either the diode or PAG with an ion current monitor of similar design to the PAG.

Injected Beam

The beam current pulse injected into the PAG (Fig. 2--10 kA peak, 40 ns FWHM) was measured with the current monitor located 50 cm from the anode. An allowance for beam debunching, due to the drop in diode voltage from 550 to 100 kV during the injector pulse, gives a proton current of 15 kA at the anode. The beam current transported to the monitor dropped by a factor of four when gas neutralization was not used. Attempts to space-charge neutralize the beam with passive and active wall electron sources gave only slight increases in the transport efficiency.

Magnetic Field Deflection Calculations

Particle trajectory simulations were performed to study the proton bending in the B_{app}-field regions near the PAG. The code conserved both canonical angular momentum and energy to calculate the angular and axial velocities. The radial velocity was determined from a sum of the centrifugal, B_{self}-field and B_z x v_a forces. An 8 kA, 400 kV proton beam with a 2.5 cm FWHM Gaussian profile centered between the coils was assumed to approximate the experimental beam parameters at peak beam power. Figure 3 shows the results of the calculations for parallel and diverging beams with and without self-B field.

PAG Operation

The centered or downstream PAG geometry gave the lowest electron leakage current in open circuit operation and was the most desirable for efficient accelerator operation. The electron loss was equal to about 3 kA with no ion beam present at a gap voltage of 350 kV and applied-B field at the outer anode-cathode gap of 6 kG (2 B_{crit}). This is to be compared to 9 kA under similar conditions when the gap was moved 4 mm upstream. When a 10 kA beam was injected into the gap, the gap current increased to 14 kA and 22 kA for the centered or downstream and upstream gap locations, respectively.

Space-Charge Neutralization

Measurements of the beam transported through the energized gap without gas puffs demonstrated the same rapid beam blow-up that was previously described for the injector. However, similar data acquired with gas puff, but without the applied-B field, showed no beam blow-up beyond that expected for ballistic transport. The latter measurements show that the beam was space-charge neutralized to within a factor of 3×10^{-5} in field free regions. Beam current measurements also showed that the beam was well current neutralized throughout the gap region when no applied-B field was present. Since the injector puff plume extended only about 20 cm downstream from the injector, this demonstrates that the space-charge neutralization problem was limited to the region of applied-B field.

Self Magnetic Field Bending

The beamlet angles determined from shadowbox data with no applied magnetic field are denoted by the circles in Fig. 4. A projection of these ray orbits to the anode of the injector confirm that a majority of the beam originates at about 1 cm from the outer cathode.

With a small value of applied-B field, current neutralization was lost over the 16 cm applied field region and the outer portion of the beam was deflected inwards ~ 1.5°. The ion beamlet angles for a 1 kG field at the outer cathode (denoted as triangles in Fig. 4) show this effect. The data lie reasonably close to the calculated deflections for B_o of 0 and 2 kG.

The self-B field also added a small amount of divergence to the beam because the beam current density was spatially non-uniform. In the present experiment, local current density enhancements of 25 A/cm^2 with 1 cm radius were observed. This yields a bending angle of 0.15° at the perimeter of such a current density enhancement.

Applied Magnetic Field Bending

Typical total B-field bending angles measured with the shadowbox system are also shown in Fig. 4. The deflection angles from the simulations for B_o ranging from 0 to 6 kG are shown as continuous curves of Fig 4. (It was necessary to modify the simulation output so that the experimental and simulation angles corresponded to the same measurement.) The data points plotted with squares in Fig. 4 were obtained with B_o of 4.5 kG and the gap filled with plasma. These data agree well with the calculated deflection curve for B_o of 4 kG near the inner cathode but are somewhat larger near the outer cathode. The discrepancy may be due to the fact that the maximum witness plate damage may occur before peak power when the beam voltage is higher than 400 kV and the current less than 8 kA.

Electrostatic Focusing Due to E x B Drifting Electrons

When voltage is applied to the PAG, additional electrostatic focusing occurs near regions of non-uniform ion beam current density. Local beam non-uniformities then appear downstream in the accelerator as "tear drop" shaped profiles. The focusing is caused by the shear between the ion and electron space-charge in the gap due to the azimuthal E x B drift of the electrons and is strongest where the beam is eliminated by the supports for the inner field coil. When voltage was applied to the gap, the beam is strongly focused on one side of each support and defocused on the other. Evidently, the electrons in the cathode sheath do not flow smoothly across the azimuthal disruption in the ion beam, but bunch up before it and drift across the gap to the anode edges. It then takes several cm of azimuthal distance before a sufficant quantity of new electrons are injected into the gap to equalize the ion beam charge. This type of electron behavior has been seen in many other experiments[4] where the sheath electrons see an abrupt change in the ion space-charge density in the E x B direction.

The tear drop effect (TDE) was most severe when the A-K gap was centered between the magnetic field coils. The data show systematic pointing errors of up to 1.5° due to the TDE from the supports. The data also show a random pointing error of ~ 0.5° that is due to local TDE in the gap and electron sheath non-uniformities attributed to cathode plasma irregularities.

Increasing the B_o field to 8 kG (3 B_{crit}) reduced local beam filamentation and the TDE near the supports considerably. Also, moving the gap upstream helped because the additional electron leakage resulted in less efficient electron trapping in the gap. Since the latter change also resulted in lower gap voltage, both changes produced a smaller E x B drift velocity and less shear between the electrons and ions. The TDE was also reduced by installing surface flashover ion sources on the anode side of the gap in the regions where the beam current was absent to provide ion space-charge to fill in the "gaps" in the current and increased the accelerating-gap ion current by a small amount.

Applied Electric Field Deflections

Experiments with a tilted gap (accomplished by moving the center coils and electrode edges downstream with respect to the outer coils and edges) demonstrated that the beam was deflected radially by the electric field in the gap. Electrostatic deflection calculations made for a gap voltage of 150 kV assuming the equipotentals were parallel to the curved B_{app}-field lines passing through the center of the gap gave reasonable agreement with the experimental deflections.

Finally, we investigated whether the curved B_{app} field lines could be used to define the equipotential surfaces in the gap. This was accomplished by moving the gap electrodes upstream and downstream with the coil positions fixed. With a centered gap and accelerating voltage of 200 kV, the beam was undeflected in the gap except for magnetic bending and space-charge deflections. The magnetic bending overcame inward and outward space-charge deflection at the edges of the beam to produce a weak focus 50 cm downstream. When the gap was moved 4 mm upstream from the midplane of the applied-B field, the beam formed a line focus at midradius from 20 to 50 cm downstream. When the gap was moved 4 mm downstream from the midplane, there were two weakly formed line foci at the edges of the beam.

Current Monitor Measurements

Total ion current measurements gave a charge transport efficiency of 80% at a B_o field of 6 kG with the gap centered or 2.5 mm upstream and tilted outward 5° (inner downstream coil moved downstream 9 mm). (The efficiency was 70% without tilt, and the field increased to 8 kG to compensate for the tilt.) This beam had a 6 kA peak current and 60 ns width at 100 cm from the injector. When the post-accelerating voltage was applied 20 ns late, the ramp on this pulse compensated for the decreasing injector voltage to give a 7.5 kA, 48 ns proton pulse at the monitor. With no accelerating voltage, the applied-B field could be used to bring the beam to a focus ~ 40 cm downstream at midradius in the accelerator annulus. Experimental data with B_o of 5 to 6 kG and no gap voltage show that 90% of the beam charge could be transported to the current monitor 50 cm downstream under these conditions. This was the most efficient transport configuration and may have occurred because

the space-charge blow-up in the gap partially cancelled excessive magnetic bending near the coils.

The ~ 20% of the beam charge lost when the gap was energized was not located with experimental techniques. However, several loss mechanisms exist. First, the protons passing near the inner coils would receive too large a deflection to arrive within the 4 cm wide acceptance annulus of the current monitor. Second, the beam in the wings of the divergence profile outside of the 4 cm wide acceptance window at the current monitor would be lost. For a 1° HWHM Gaussian beam divergence profile, that loss would be 18% of the beam. This gives an upper bound on the divergence and suggest the divergence is much smaller than 1°. Third, some current is lost because of residual beam distortion near the coil supports.

Conclusion

The dominant beam deflection physics relevant to multi-gap accelerator operation has been examined. We determined that space-charge neutralization is inadequate without a background gas or plasma fill in the B_{app}-field regions. We find that the beam was not current neutralized in B_{app}-field regions leading to significant B_{self}-field bending. In addition, we observed several degrees of radial focusing that occurs because of the solenoidal focusing of the applied field coils. Along with the demonstrated electrostatic focusing from the PAG, this provides a mechanism for radial beam confinement during transport in multi-gap accelerators.

We also observed local electrostatic deflections in the PAG that add to the beam emittance. These deflections are initiated by spatial non-uniformities in the beam and occur due to non-axisymmetric space-charge blow-up and shear between the beam ions and electrons in the cathode sheath caused by the E x B drift of the electrons. The data obtained indicate emittance from E x B effects can be kept from growing indefinitely during multi-gap operation if the applied-B field is approximately 3 B_{crit}.

References

1. S. Humphries, Jr., Nucl. Fusion 20, 1549 (1980).
2. T. R. Lockner, S. Humphries, Jr., and J. J. Ramirez, IEEE Trans. Nucl. Sci. NS-28, 3407 (1981).
3. D. J. Johnson, J. P. Quintenz, and M. A. Sweeney, J. Appl. Phys. 57, 794 (1985).
4. D. J. Johnson, E. J. T. Burns, J. P. Quintenz, K. W. Beig, A. V. Farnsworth, Jr., L. P. Mix, and M. A. Palmer, J. Appl. Phys. 52, 168 (1981).

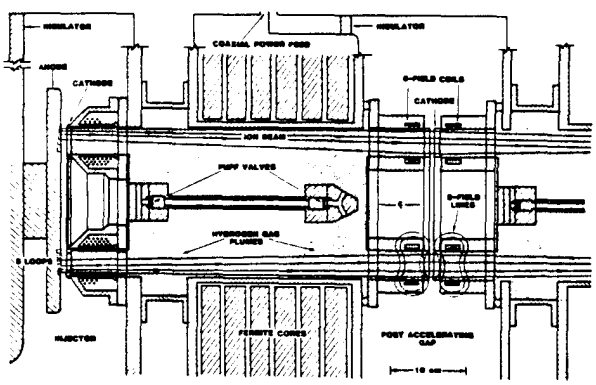

Figure 1. Pulselac injector and PAG.

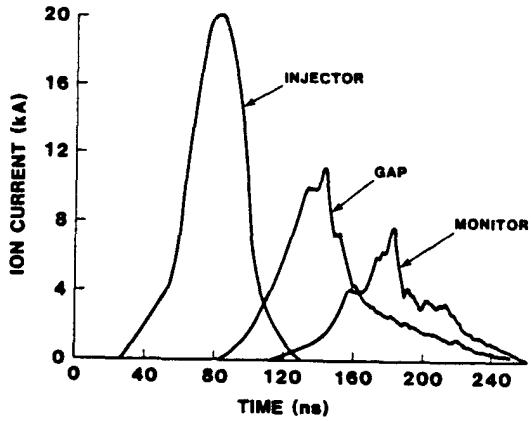

Figure 2. Total ion current as measured at injector, PAG, and 50 cm from PAG. Trace labeled "monitor" shows some pulse compression due to PAG voltage.

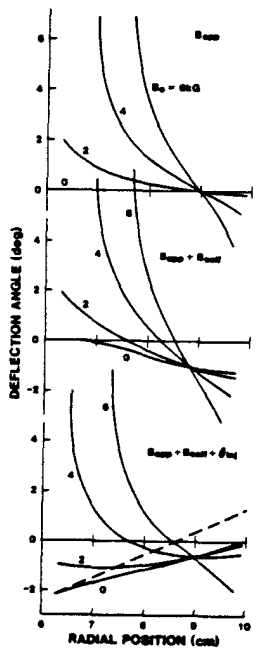

Figure 3. Simulations of self and applied magnetic field deflection from PAG. Lowest figure includes injected beam angle (dotted line).

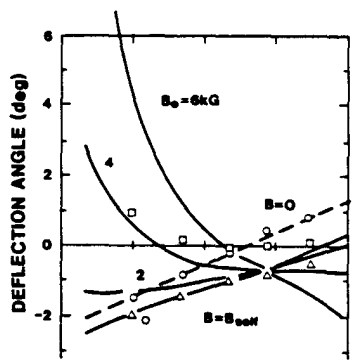

Figure 4. Self and applied field bending data. Solid lines are simulation output, circles for no field (incident angle). Note for small applied field (triangles), there is significant self-field bending. At larger applied field, solenoidal focusing is also evident (squares).